Journal of the Serbian Society for Computational Mechanics / Vol. 17 / No. 2, 2023 / pp 87-103
(10.24874/jsscm.2023.17.02.07)

BEHAVIOR OF NON-NEWTONIAN FLUID IN A LID-DRIVEN CHAMBER WITH HEATED BODIES SUBJECTED TO A UNIFORM MAGNETIC FIELD

Yamina Anouar

Department of Hydraulics, University of Science and Technology of Oran – Mohammed Boudiaf, B.O. Box 1505, El-M'Naouer, 31000, Oran, Algeria
e-mail: yaminaa833@gmail.com

Abstract

Recent studies have attempted to find methods and techniques that enable the development of heat transfer within thermal transformers. For this purpose, this paper includes a numerical simulation of a non-Newtonian fluid inside a chamber with four hot bodies. The chamber is exposed to a magnetic field of constant and uniform intensity. Also, the upper wall of the chamber has a horizontal movement. The study is based on the quality of heat transfer between the heated parts of the chamber and the complex fluid under the influence of a set of criteria, namely Reynolds number (= 1 to 40); Hartmann number (= 0 to 100); power-law index (= 0.6 to 1.4) and Richardson number (0 to 100). The interpretation of the results is done by displaying the path-lines and isotherms distribution. Also, the amount of thermal transfer of the hot bodies is given in terms of the Nusselt number. The results showed that the positioning of the hot bodies plays an important role in heat transfer. Moreover, increasing the value of the power-law index makes the fluid stickier, which reflects its negative effect on heat transfer.

Keywords: Non-Newtonian fluid, MHD, fluid mechanics, hot bodies, mixed convection.

1. Introduction

All studies related to thermal activity aim to find possible solutions to accelerate heat transfer. A thermal system often consists of hot and cold elements immersed in a fluid such as air, water or some other type of fluid (Al-Kouz et al., 2021; Laidoudi, and Bouzit, 2017a; Hussain et al., 2019). It can be said that thermal systems are present in all industries and technology applications such as high-precision cooling systems, heat exchangers, nuclear stations, solar energy systems and other applications.

Based on the previous definition of the thermal system, the studies in this regard are divided into two parts. The first section is concerned with the geometry of the thermal system and geometric modifications that allow the development of heat transfer (Aliouane et al., 2021; Mokeddem et al., 2019; Henry et al., 2017; Lorenzini et al., 2016). As for the second type of studies, it is based on the kind of fluid and its thermal properties that can accelerate the thermal activity of the system under study (Sheikholeslami and Oztop, 2017; Sheikholeslami et al., 2016;

Zhang and Che, 2016; Matin et al. 2013; Laidoudi and Bouzit, 2017b; Jamshed et al., 2022; Bendrer et al., 2021; Prhashanna and Chhabra, 2010).

For the first type of studies, (Liao and Lin, 2012) provided a study on the free and mixed thermal activity in a closed container. The results of this work show the effect of the geometric shape of the solid body on the fluid pattern and thermal transfer. There are also other geometrical configurations taken into account. Yuce and Pulat (2018) conducted a digital and experimental study of heat distribution inside a triangular chamber. As for the digital results, they used many models that define the turbulent patterns of the fluid flow. In addition to this, some geometric changes have been proposed and achieved for the purpose of evaluating thermal activity.) Some numerical studies focused on the evolution of thermal activity within systems of different geometries (Laidoudi and Bouzit, 2018; Laidoudi, 2020; Laidoudi and Bouzit, 2017c; Laidoudi et al., 2022a). These studies show the effect of many parameters on thermal transfer, but primarily on the geometry of the system. The studies have shown that there is an effect of the geometric shape on the performance of the thermal system. Torres et al. (2020) conducted a study to determine the thermal activity emitted from a hot body with blades subject to ambient air. The flow has high speed which makes it turbulent. In addition to this, the body was done according to changing the position of that body inside the channel. The results depicted the importance of the geometry of the hot body on the quality of thermal activity. Furthermore, there are also important geometric shapes that have been studied in order to develop the thermal system (Burgos et al., 2016; Mandal et al., 2023; Luo et al., 2014; Yadav et al., 2022; Abdel-Nour et al., 2020). Most of these studies confirm that the shape of a thermal system is the first factor that determines the nature of thermal activity and its effectiveness in thermal transfer.

For the second type of studies, this type of research is based on the discovery of high thermal performance fluids. The thermal properties are expressed by the Prandtl number; the higher the value of this number, the higher the thermal properties of the fluid, which accelerates the transfer of thermal energy. This is a group of works that illustrate the aforementioned conclusion (Koca et al., 2008; Baranwal and Chhabra, 2016; Al-Amir et al., 2019; Laidoudi and Ameur, 2020). On the other hand, some other works resorted to the use of non-Newtonian fluids to develop thermal activity (Kefayati, 2015; Molla and Yao, 2009; Laidoudi et al., 2021, 2020; Guendouci et al., 2021; Mahdy et al., 2010). These types of fluids are distinguished by their ability to change their viscosity, which allows a change in their heat transfer properties. In addition to this, a new type of fluid called nanofluid has been recently introduced. This fluid consists of ordinary water with particles of fine solid bodies called nanoparticles added to it. The additives improve the thermal properties of the fluid while not significantly altering the hydrodynamic properties. For this reason, many new works use this kind of fluid in order to expand knowledge about it (Selimefendigil and Öztop, 2018; Chen et al., 2015; Aissa et al., 2023; Laidoudi et al., 2022b; Jamaludin et al., 2021). Also, there is a type of fluid called NEPCM (Aissa et al., 2022a; Sadr et al., 2022; Aissa et al., 2022b; Ghalambaz et al., 2019; Aly et al., 2022), which is one of the manufactured fluids. This kind of suspension is composed of water and very fine capsules. Inside these capsules, there is a solid substance that turns into a liquid when it absorbs enough heat. That is, these capsules can absorb a high amount of heat compared to solid bodies used in nanofluids.

Based on the above research, this work aims to add new results about the thermal activity of the complex fluid in a lid-driven chamber containing four hot bodies, under the influence of the magnetic field factor and the phenomenon of thermal buoyancy. The results of this work can be used in the development of a small-sized thermal exchanger for electronic applications such as CPU.

2. Description of the studied domain

Figure 1 presents a simplified form of the studied system. The system consists of four hot circular bodies inside a square container. The side walls are cold and have three fins. As for the lower wall, it is adiabatic, while the top side is also adiabatic and has a horizontal movement from left to right. The inner space of the chamber is filled with non-Newtonian liquid known mainly by the index (n). Furthermore, an external field of magnetic (B0) is applied to the exchanger. The geometric dimensions of this exchanger are L = 100 (mm) and d/L = 0.1. The thermal characteristics of the working fluid are given by Prandtl number (Pr = 50).

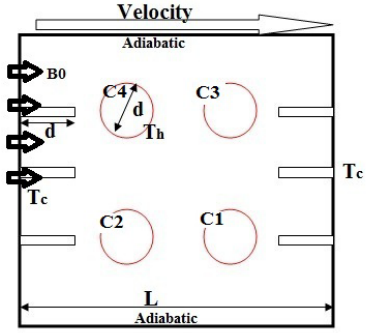

Fig. 1. Domain under consideration.

The following considerations were used to simulate the present study: the Boussinesq approximation was selected for coupling the velocity flow and temperature; the Ostwald model was used to describe the rheological behavior of the liquid, while Joule heating and displacement currents were neglected. The appropriate governing equations for the present study in the Cartesian coordinate system are:

$$\frac{\partial u}{\partial x}+\frac{\partial v}{\partial y}=0 \tag{1}$$

$$u\left(\frac{\partial u}{\partial x}\right)+v\left(\frac{\partial u}{\partial y}\right)=-\frac{1}{\rho}\frac{\partial p}{\partial x}+\frac{1}{\rho}\left(\frac{\partial \tau_{xx}}{\partial x}+\frac{\partial \tau_{xy}}{\partial y}\right)+\frac{\sigma B_0^2}{\rho}\left(v\sin(\gamma)\cos(\gamma)-u\sin^2(\gamma)\right) \tag{2}$$

$$u\left(\frac{\partial v}{\partial x}\right)+v\left(\frac{\partial v}{\partial y}\right)=-\frac{1}{\rho}\frac{\partial p}{\partial y}+\frac{1}{\rho}\left(\frac{\partial \tau_{xy}}{\partial x}+\frac{\partial \tau_{yy}}{\partial y}\right)+\frac{\sigma B_0^2}{\rho}\left(u\sin(\gamma)\cos(\gamma)-v\sin^2(\gamma)\right)+\beta g(T-T_c) \tag{3}$$

$$u\left(\frac{\partial T}{\partial x}\right)+v\left(\frac{\partial T}{\partial y}\right)=\alpha\left(\frac{\partial^2 T}{\partial x^2}+\frac{\partial^2 T}{\partial y^2}\right) \tag{4}$$

The Ostwald model describes the dynamic viscosity in complex fluid by the following:

$$\tau_{ij}=m\left(2\left[\left(\frac{\partial u}{\partial x}\right)^2+\left(\frac{\partial v}{\partial y}\right)^2\right]+\left(\frac{\partial u}{\partial x}+\frac{\partial v}{\partial y}\right)^2\right)^{(n-1)/2}\left(\frac{\partial u_i}{\partial x_j}+\frac{\partial u_j}{\partial x_i}\right) \tag{5}$$

where (m) indicates the factor of consistency, while (n) is power-law index. The symbols (i and j) are component e i, j-directions of the coordinate axis. If (n > 1), the dynamic viscosity of the liquid augments as the friction factor of the flow augments. If (n < 1), the dynamic viscosity of the liquid decreases as the frictional factor augments. If (n = 1), the dynamic viscosity does not

depend on the frictional coefficient. Generally, the values studied of the power-law index are specific to some composite industrial fluids such as polymers.

The fluid properties with the studied system are controlled by non-dimensional numbers given as follows: Prandtl number ($Pr = mC_p/k(u_{in}/L)^{n-1}$) in order to determine the thermal properties; Reynolds number ($Re = \rho(u_{in})^{2-n}L^n/m$) in order to determine the rotational speed of the circular chamber; Grashof number ($Gr = g\beta_T\Delta TL^3[\rho/m(u_{in}/L)^{1-n}]^2$) in order to determine the thermal buoyancy force; Richardson number ($Ri = Gr/Re^2 = g\beta_T\Delta TL^3/(u_{in})^2$) in order to know the ratio between the natural convection over the forced convection. Hartman number ($Ha = LB_0(\sigma/\mu)^{1/2}$) in order to determine the magnetic field. The dynamic viscosity in this case can be calculated as: $\mu = m(I_2/2)^{(n-1/2)}$.

Dimensional boundary conditions with an appropriate form are used for the studied system:

- On the heated walls of obstacles: $u = v = 0, T = T_h$
- On the cold side chamber: $u = v = 0, T = T_c$
- On the down wall chamber: $u = v = 0, \dfrac{\partial T}{\partial ns} = 0$
- On the cold side chamber: $u = u_{in}, v = 0, \dfrac{\partial T}{\partial ns} = 0$

The local and average values of Nusselt number are given as:

$$Nu_L = \left(\frac{\partial T}{\partial ns}\right)_{wall} \text{ and } Nu = \frac{1}{A}\int_s Nu_L dA \tag{6}$$

3. Solution methodology and code validation

The present simulations are done using ANSYS-CFX simulator. The latter converts the governing equations (of differential form) into a matrix system. And by exerting the boundary conditions, solutions are solved using the method of the finite volume. The simulation results take into account that the error factor is less than the value 10^{-6} for the three governing equations. However, high resolution schema was adopted for calculating the convective terms. On other hand, pressure-velocity coupling was adopted by SIMPLEC algorithm.

Currently, we confirm that the number of grid elements has influence on the solving method. Therefore, four grids were generated with augmenting density in the number of grid elements, after which the value of the Nusselt number was computed for the four cylinders in each case. The results of this test and the number of grid elements are presented in Table 1. Through Table 1, it is possible to deduce that there is stability in the values of the Nusselt number for the four cylinders when the grid elements exceed the value 653,600. Therefore, this number is sufficient to calculate accurate values.

Gird	elements	Nu (C1)	Nu (C2)	Nu (C3)	Nu (C4)
G1	188,388	27.3620	18.2134	15.4344	15.3221
G2	376,775	29.2323	20.1897	15.9889	18.4884
G3	653,600	**30.2213**	**21.2334**	**16.5431**	**19.2342**
G4	1507,100	30.2112	21.3102	16.5564	19.2219

Table 1. Variation of Nu versus grid elements for Ha = 0, Re = 30, Ri = 25 and n = 1.

This part also shades a study that proves the ability of the used method to solve differential equations accurately. Therefore, we compare the results of a previous work (Sarris et al., 2006) under the same initial conditions. The comparison results are shown in Fig. 2, which shows a strong match between the results, and this indicates the accuracy of this method. A comparative study was done about a fluid enclosed in a square chamber. The left wall of the chamber is cold, and the right wall is hot. The study was achieved for Ha = 25 and 100 at Ra = 7.10^5.

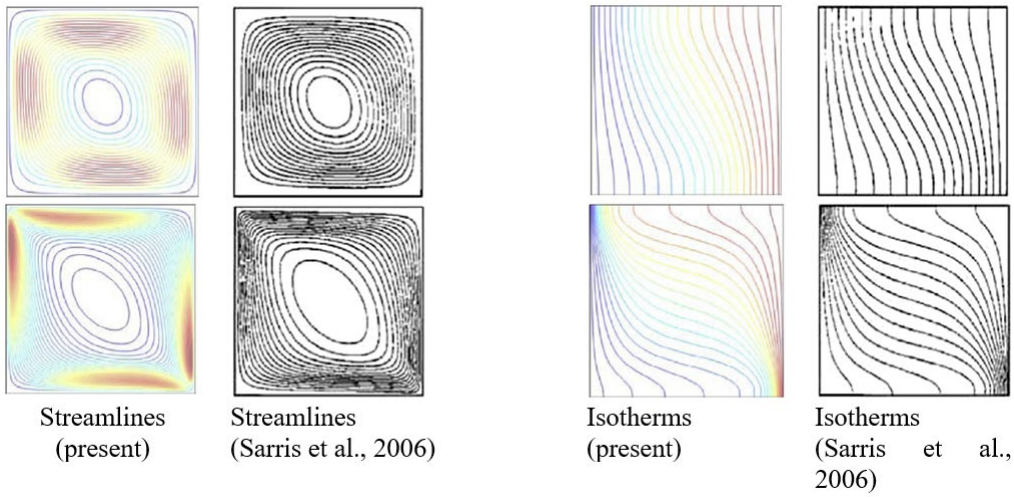

Fig. 2. Validation code for Ha = 25 and 100 at Ra = 7.10^5.

Figure 3 shows a comparison of the values of Nu number in terms of Ha number for power-law index n = 1.4, Ra = 10^5. Comparison results are taken from (Kefayai, 2016) work. It is noted that there is a similarity between the results, and this is what strengthens the method used. A comparative study was conducted around a square chamber containing a complex fluid with power-law index of n = 1.4 and with the effect of the magnetic field. The results were calculated in terms of Hartmann number for Ra = Ra = 10^5.

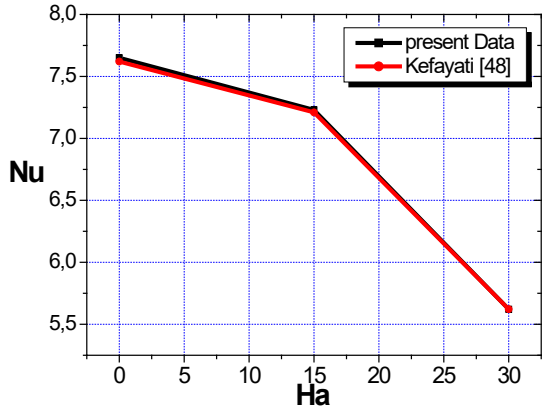

Fig. 3. Comparing the value of Nu of (Kefayai, 2016) in terms of Ha for Ra = 10^5 and n = 1.4.

4. Results and discussion

This research aims to deduce the heat transfer process of four hot bodies placed inside a room containing a non-Newtonian fluid. The chamber has two cold walls (left and right), while the upper wall is movable and thermally insulated; the lower wall is fixed and adiabatic as well. Some factors affecting the thermal transfer between hot bodies and cold walls have been studied. These factors are the non-Newtonian properties of the fluid, the intensity of buoyancy, the speed movement of the upper wall and the magnetic field strength applied externally to the chamber. To examine the thermal and dynamic behavior of the fluid particles, isotherms, and pathlines were shown in terms of the studied factors. As for the qualitative values of thermal transfer, they were presented in terms of Nusselt number.

Figure 4 depicts the pathlines and dimensionless temperature in the cavity in terms of power-law index (n) for Re =40, Ha = 0 and Ri = 50. These values refer to the horizontal movement of the upper side from left to right with the presence of the effect of thermal buoyancy of the hot fluid and in the absence of the magnetic field because Ha = 0. It is noted in Fig. 3 that the pathlines are formed by the combination of horizontal movement of the upper wall and vertical movement due to thermal buoyancy. Because the hot spots of the fluid become less dense and thus shift upwards. It is also noted that the contours of dimensionless temperature refer to this analysis. That is, the cold spots of the fluid are concentrated at the bottom of the cavity, while the hot spots are at the top. With regard to the effect of factor (n), it is noted that the higher this index, the movement of the flow inside the room becomes circular, that is, it follows the movement of the upper wall, and a decline in the temperature gradient around the hot bodies is observed. This pattern indicates a decline in the heat transfer of the hot bodies in terms of power-law index. From a physical point of view, this can be explained by the following: an increase in the index (n) indicates that the rheological nature of the fluid changes, that is, the effect of the viscosity of the fluid increases, which makes the fluid resistance higher for movement. Therefore, a decrease in thermal activity was observed due to the decrease in the speed of the flow. In addition to this, it is noted that the temperature gradient around the two bodies located at the bottom is higher than those at the top, which means that the heat transfer for them is higher.

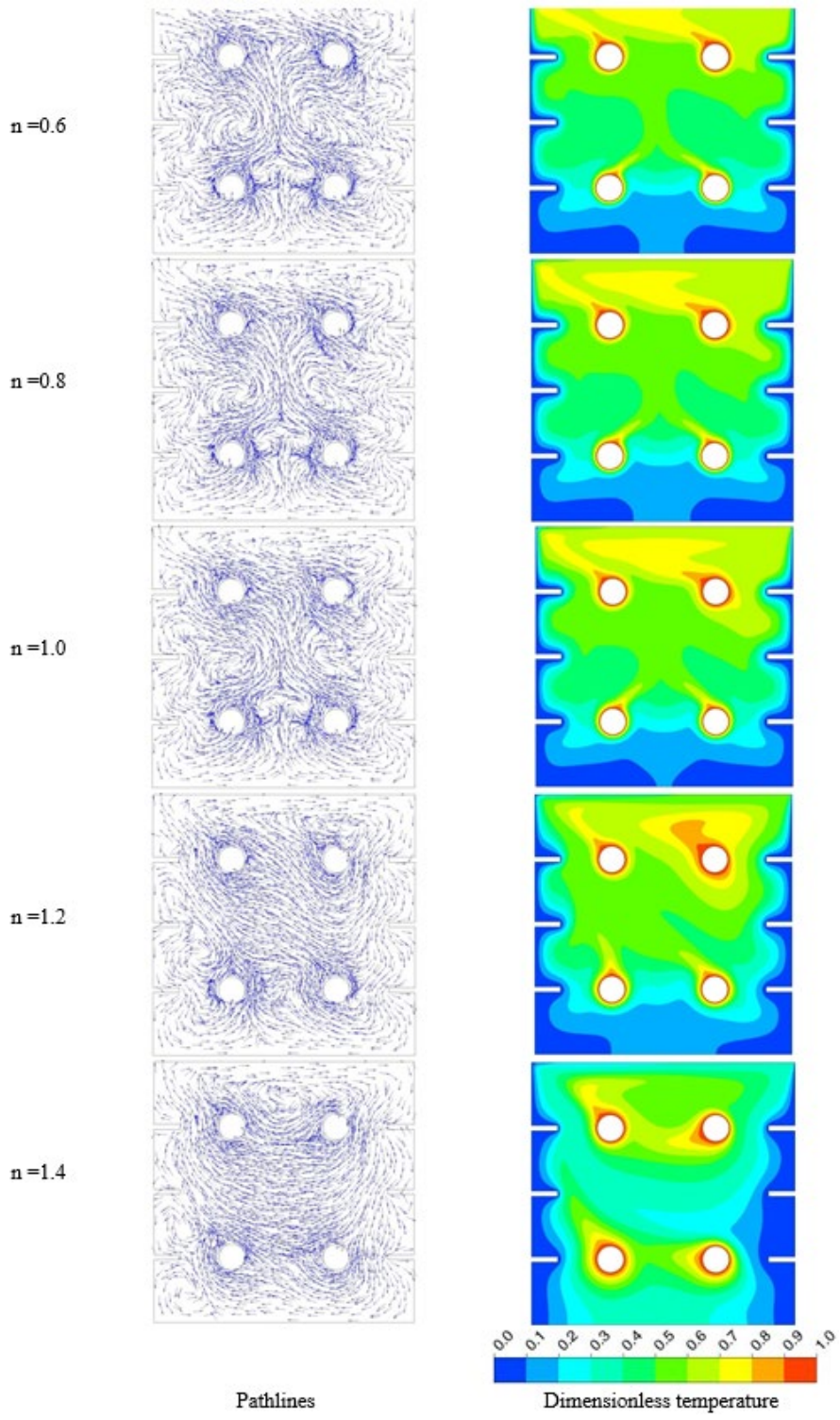

Fig. 4. Pathlines and dimensionless temperature in terms of power-law index for Re =40, Ri = 50 and Ha = 0.

Figure 5 shows evolutions of the Nusselt number for all hot bodies (C1, C2, C3, and C4) in terms of the power-law index (n) for Re =40, Ri = 50 and Ha = 0. In general, it is noted that increasing the power-law index negatively affects the Nusselt number for all hot bodies. This, of course, is due to the viscosity property, which makes the movement of the flow more difficult and thus reduces the effectiveness of the flow in transferring thermal energy. On the other hand, it is noted that the two bodies at the bottom have higher values for the Nusselt number.

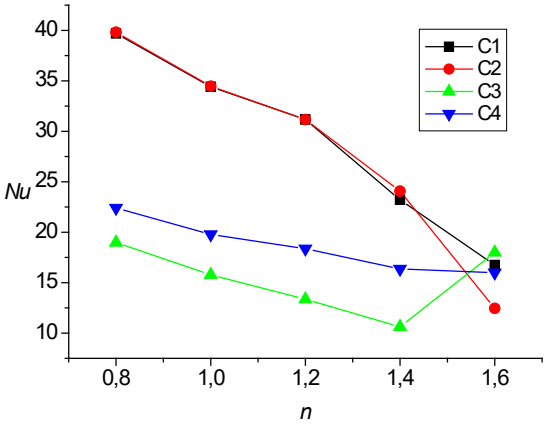

Fig. 5. Variation of Nusselt number versus power-law index for four bodies at Re =40, Ri = 50 and Ha = 0.

Figure 6 shows the contours of pathlines and dimensionless temperature inside the chamber in terms of the gradual augmentation of the Reynolds number from 1 to 40 and for n =1, Ri =1 and Ha = 0. An increase in this number indicates an increase in the speed of movement of the upper wall of the container. It is noted that the higher the value of this number (Re), the greater the expansion of the fluid diffusion inside the chamber, and this is accompanied by a change in gradient temperature around the hot bodies. That is, the heat transfer from the hot objects increases and this is mainly due to the movement of the upper wall, because its movement increases the speed of the fluid particles, and this is what develops the thermal activity. However, it is also concluded from Fig. 6 that heat transfer differs from one body to another due to the movement of the flow.

Figure 7 represents evolutions of the values of the Nusselt number for hot bodies in terms of the Reynolds number for n =1, Ri =1 and Ha = 0. These parameters indicate that the fluid is Newtonian (n = 1) and the effect of thermal buoyancy is small (Ri = 1), with the absence of the magnetic field (Ha = 0). It is observed here that increasing the Reynolds number positively affects all hot bodies. The arrangement of these hot bodies in terms of their Nusselt number values is as follows: C1, C3, C4 and C2. This arrangement is due to little effect of thermal buoyancy, and because the movement of the flow is from the right towards the left.

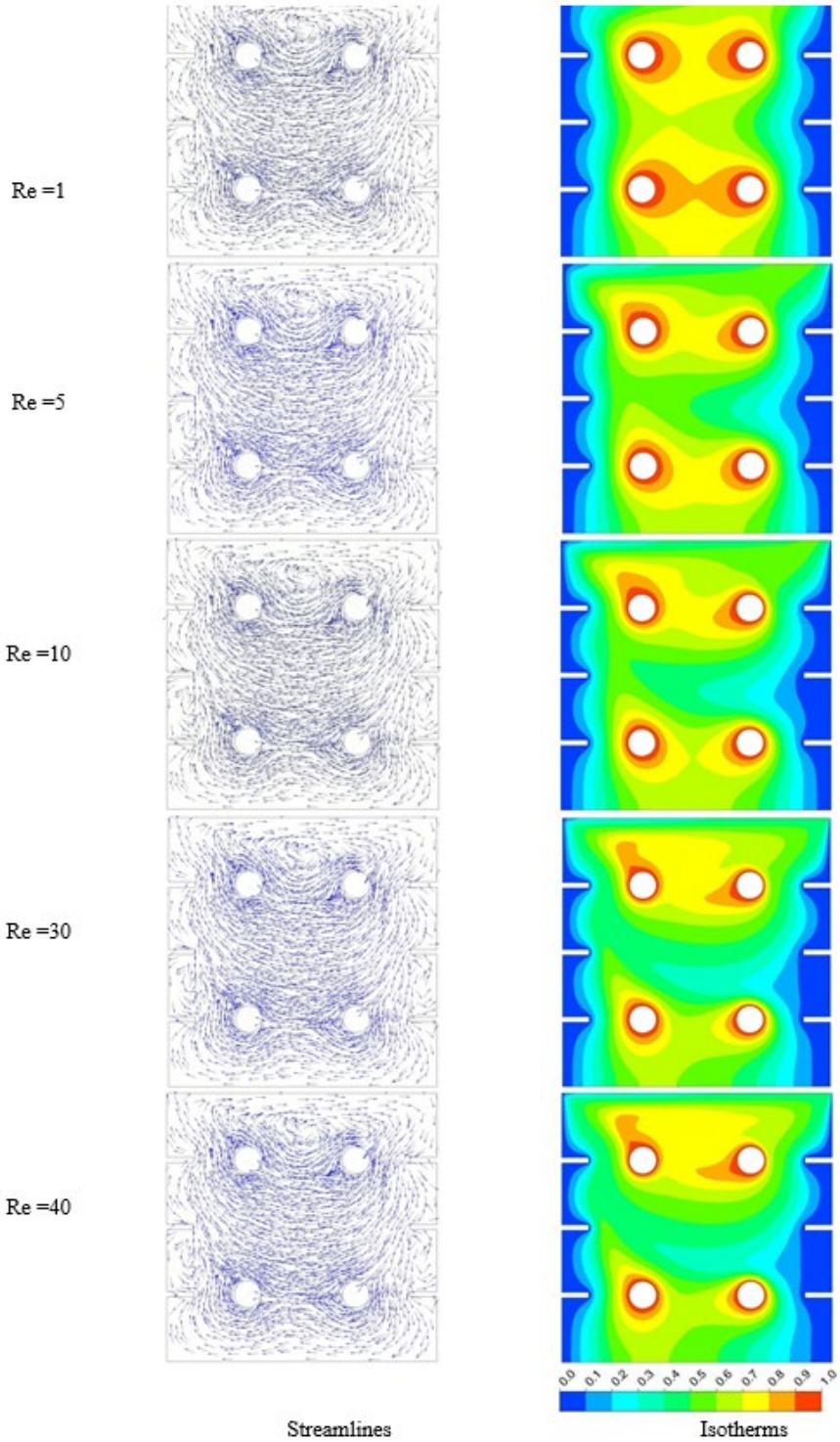

Fig. 6. Pathlines and dimensionless temperature in terms of Reynolds number for n =1, Ri =1 and Ha = 0.

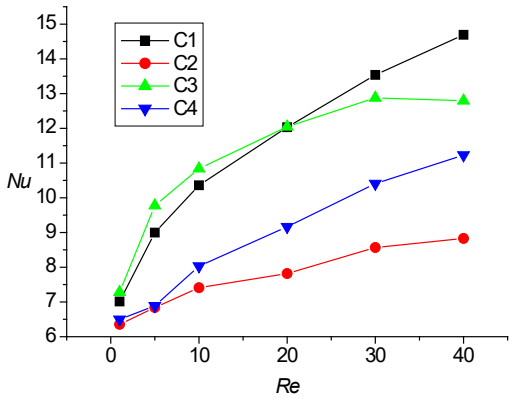

Fig. 7. Variation of Nusselt number versus Reynolds number for four bodies at n =1, Ri =1 and Ha = 0.

Figure 8 represents the evolution of the pathlines and dimensionless temperature in terms of the gradual increase of Richardson number for n =1, Re=40 and Ha = 0. An increase in the value of the Richardson number means an increase in the temperature of the hot bodies, so the effect of the thermal buoyancy force increases. Increasing the intensity of thermal buoyancy means that the hotter fluid spots rapidly rise upward while the colder spots become condense and heavier and thus move downwards. Therefore, the motion diagrams show the fluid moving upwards as it is hot, while on the cold walls its direction is downward. In addition to this, since the cold fluid is focused on the bottom, it means that the thermal activity of the two lower bodies is higher than that of the two upper bodies. Also, the presence of fins on the cold walls brings the cold fluid spots closer to the hot bodies.

Figure 9 depicts the evolution of the values of Nusselt number for each hot body separately in terms of Richardson number for n = 1, Ha = 0 and Re = 40. We note that increasing the value of the Richardson number gradually increases the values of the Nusselt number for all hot bodies due to the increase in the velocity of the flow inside the chamber. Also, the mean values of the Nusselt number of the two lower bodies are higher than those of the two upper bodies. Due to the concentration of cold spots of the fluid at the bottom.

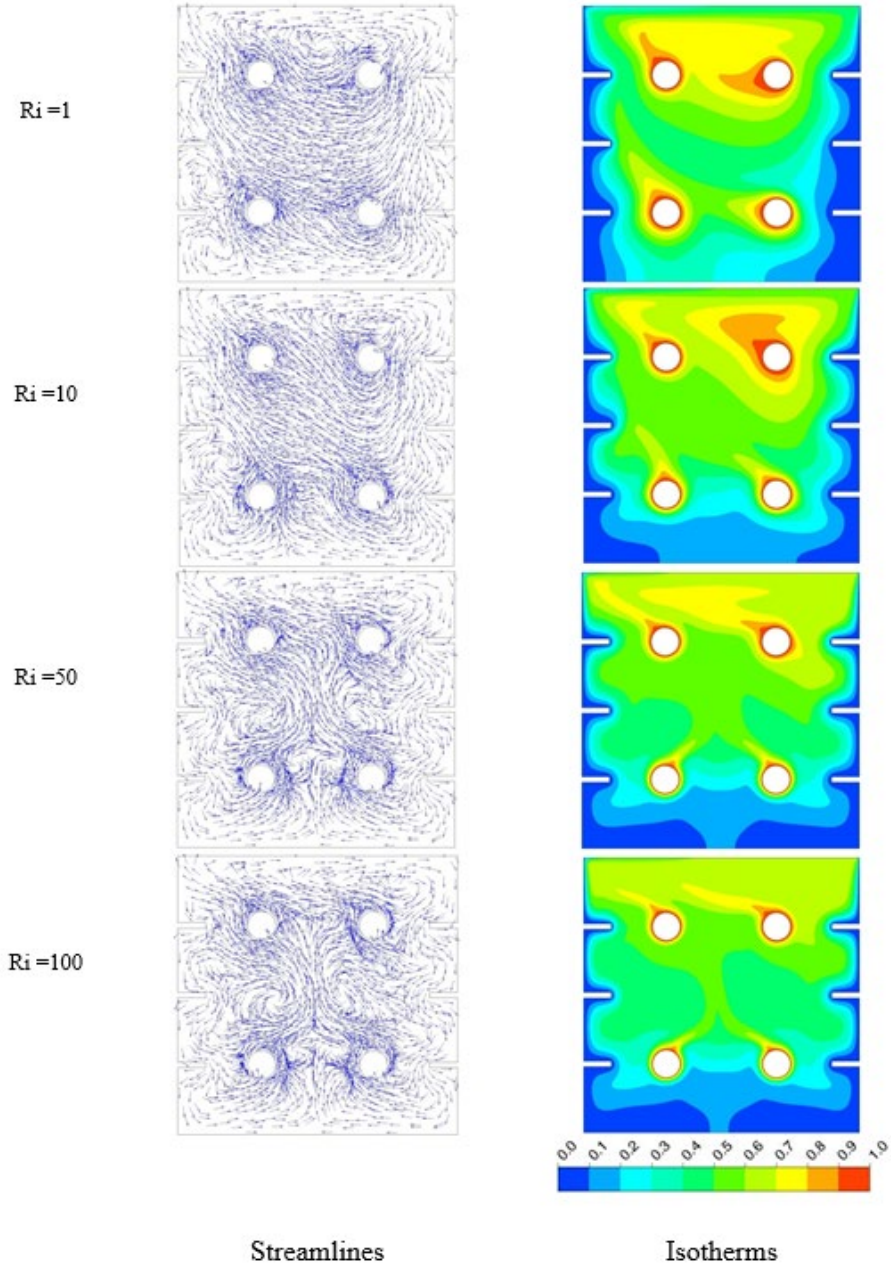

Fig. 8. Pathlines and dimensionless temperature in terms of Richardson number for n =1, Re = 40 and Ha = 0.

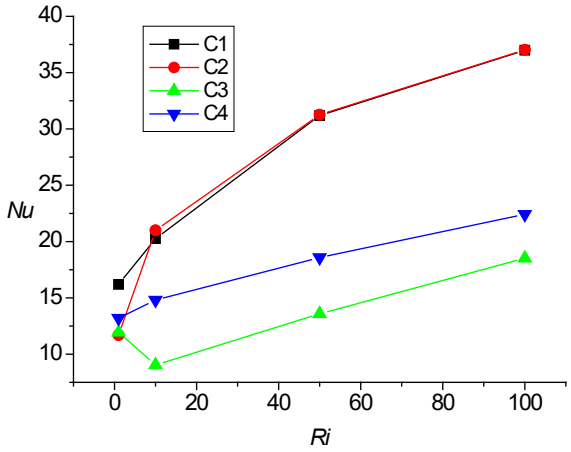

Fig. 9. Variation of Nusselt number versus Reynolds number for four bodies at n = 1, Re = 40 and Ha = 0.

Figure 10 represents the evolution of the streamline and dimensionless temperature in terms of the Hartmann number (Ha) for n = 1, Re = 40 and Ri = 50. Increasing the value of this number from 0 to 100 means increasing the strength of the magnetic field. On the other hand, applying a magnetic field to a moving charge generates a force called the Lorentz force, usually in the opposite direction of the motion. It is clear from Fig. 10 that there is a decline in the flow movement inside the chamber as the value of Ha increases. Also, a decrease in gradient of temperature around the hot elements, which means a decrease in heat transfer. In addition to this, it can be concluded from this point that the magnetic field is an external factor that can control the speed of the flow and thermal activity. Furthermore, the density of the temperature gradient around the lower bodies is higher than around the upper bodies, which indicates that the heat transfer of the lower bodies is higher in the presence of the magnetic field.

Figure 11 depicts the evolution of the values of Nusselt number for four bodies (C1, C2, C3 and C4) in terms of Hartmann number for Ri = 50 and Re = 40. Fig. 11 (A) is for shear-thinning fluid (n = 0.8), Fig. 11 (B) is for Newtonian fluid (n = 1) and Fig. 11 (C) is for shear-thickening fluid (n = 1.6). It is noted first that the gradual increase in the number Ha leads to a decrease in the values of Nu of all four bodies and for all values on the index (n). This is due to the Lorentz force, which impedes the movement of the flow, and thus a decrease in flow velocity accompanied by a decrease in heat flux. In addition to this, it is noted that for n = 0.8 and 1, the maximum values of Nu are for the two lower bodies (C1 and C2). Whereas, for n = 1.6, the maximum values of this number become for the upper bodies (C3 and C4). In this case, the value of dynamic viscosity becomes high in front of the upper movable wall, and for this reason, the flow velocity is high near the two upper bodies, and therefore, the heat transfer of the upper obstacles becomes stronger.

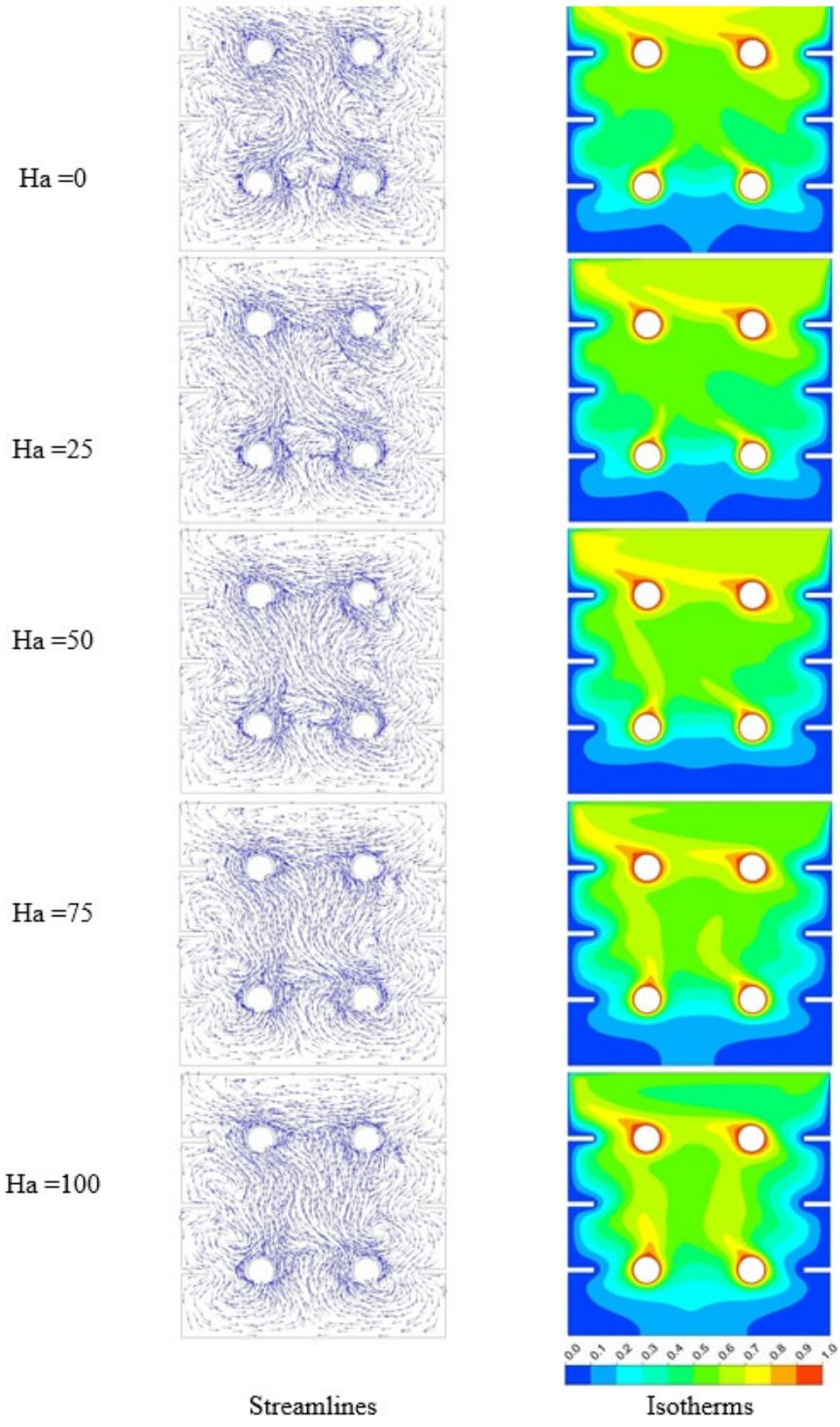

Fig. 10. Pathlines and dimensionless temperature in terms of Hartmann number for n =1, Re=40 and Ri = 50.

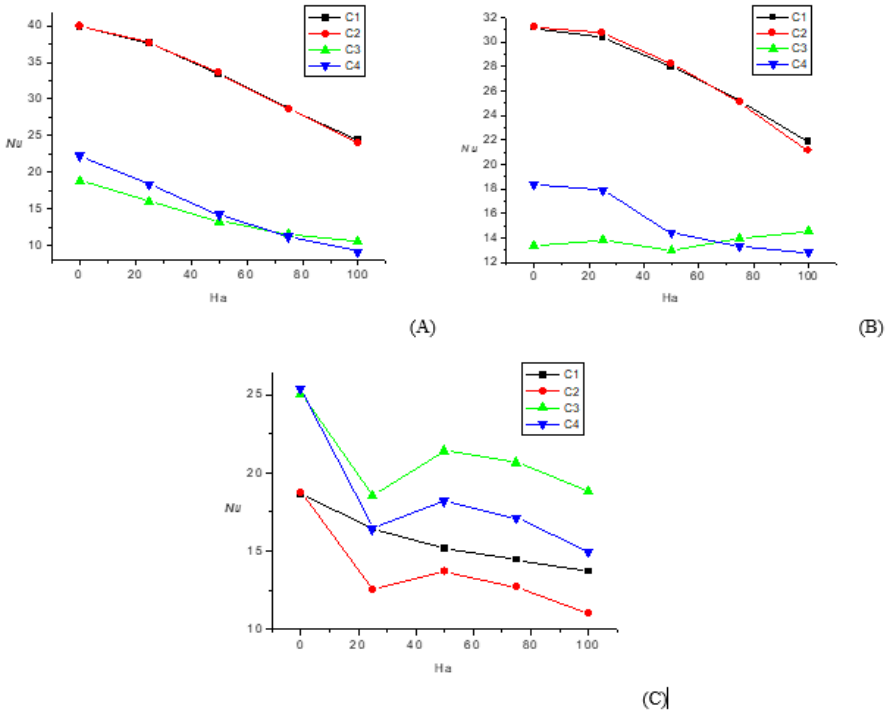

Fig. 11. Variation of Nusselt number versus Hartmann number for four bodies at n =1, Re=40 and Ri = 50. (A) for n = 0.8. (B) for n = 1.0. (C) for n = 1.6.

5. Conclusion

The study includes a numerical simulation of a complex fluid in a lid-driven chamber containing four heated bodies and subjected to a constant magnetic field. In order to enlarge the touching area between the fluid and the cold walls, some fins were added on the side walls of the chamber. The study included an examination of the impact of the following parameters: the power-law index (n) that determines the fluid's complex nature; Reynolds number which controls the velocity of the upper wall; Hartmann number that gives the intensity of the magnetic field and Richardson number that determines the force of thermal buoyancy. The study enabled us to deduce the following points:

- The position of the hot bodies is very important for the quality of heat transfer.
- Increasing the value of the Hartmann number makes the movement of the fluid particles slower, which reduces the heat transfer.
- Increasing the value of the Reynolds number makes the velocity of the upper wall faster, which enhances the thermal activity of all hot bodies.
- The higher the value of the Richardson number, the greater the thermal activity of the lower bodies.
- Increasing the power-law index negatively affects the heat transfer of all hot bodies.

- The effect of magnetic field on the heat transfer of hot bodies decreases as the value of power-law index increases.

In the future, we propose to increase the upper wall movement speed with the increase in the intensity of the thermal buoyancy force, and to make a numerical simulation related to the time (unsteady simulation).

References

Abdel-Nour Z, Aissa A, Mebarek-Oudina F, Rashad A M, Ali H M, Sahnoun M, El Ganaoui M, (2020). Magnetohydrodynamic natural convection of hybrid nanofluid in a porous enclosure: numerical analysis of the entropy generation. Journal of Thermal Analysis and Calorimetry, 141, 1981–1992.

Aissa A, Al-Khaleel M, Mourad A, Laidoudi H, Driss Z, Younis O, Guedri K, Marzouki R (2022a), Natural convection within inversed T-shaped enclosure filled by nano-enhanced phase change material: Numerical investigation. Nanomaterials, 12, 2917.

Aissa A, Qasem N A A, Mourad A, Laidoudi H, Younis O, Guedri K, Alazzam A, (2023). A review of the enhancement of solar thermal collectors using nanofluids and turbulators. Applied Thermal Engineering, 220, 119663.

Aissa A, Younis O, Al-Khaleel M, Laidoudi H, Akkurt N, Guedri K, Marzouki R, (2022b). 2D MHD mixed convection in a zigzag trapezoidal thermal energy storage system using NEPCM. Nanomaterials, 12, 3270.

Al-Amir Q R, Ahmed S Y, Hamzah H K, Ali F H, (2019). Effects of Prandtl number on natural convection in a cavity filled with silver/water nanofluid-saturated porous medium and non-Newtonian fluid layers separated by sinusoidal vertical interface. Arabian Journal for Science and Engineering, 44, 10339-10354.

Aliouane I, Kaid N, Ameur H, Laidoudi H, (2021). Investigation of the flow and thermal fields in square enclosures: Rayleigh-Bénard's instabilities of nanofluids, Thermal Science and Engineering Progress, 25, 100959.

Aly A M, Alsedias N, Galal A M, (2022). The conformable fractal systems of natural convection in an annulus suspended by NEPCM. International Communications in Heat and Mass Transfer, 134, 106023.

Al-Kouz W, Aissa A, Koulali A, Jamshed W, Moria H, Nisar K S, Mourad A, Abdel-Aty A H, Khashan M M, Yahia I S, (2021). MHD darcy-forchheimer nanofluid flow and entropy optimization in an odd-shaped enclosure filled with a (MWCNT-Fe3O4/water) using galerkin finite element analysis. Scientific Reports, 11, 22635.

Baranwal A K, Chhabra R, (2016). Effect of Prandtl number on free convection from two cylinders in a square enclosure. Heat Transfer Engineering, 37, 545-556.

Bendrer B A I, Abderrahmane A, Ahmed S E, Raizah Z A S, (2021). 3D magnetic buoyancy-driven flow of hybrid nanofluids confined wavy cubic enclosures including multi-layers and heated obstacle. International Communications in Heat and Mass Transfer, 126, 105431.

Burgos J, Cuesta I, Salueña C, (2021). Numerical study of laminar mixed convection in a square open cavity, International Journal of Heat and Mass Transfer, 99, 599-612.

Chen C K, Chen B S, Liu C C, (2015). Entropy generation in mixed convection magnetohydrodynamic nanofluid flow in vertical channel. International Journal of Heat and Mass Transfer, 91, 1026-1033.

Ghalambaz M, Groşan T, Pop I, (2019). Mixed convection boundary layer flow and heat transfer over a vertical plate embedded in a porous medium filled with a suspension of nano-encapsulated phase change materials. Journal of Molecular Liquids, 293, 111432.

Guendouci I, Laidoudi H, Bouzit M (2021). The effect of fin length on free convection heat transfer in annular space of concentric arrangement using shear-thinning fluids as a thermal medium, Defect and Diffusion Forum, 409, 194-204.

Henry R, Tiselj I, Matkovič M, (2017). Natural and mixed convection in the cylindrical pool of TRIGA reactor. Heat and Mass Transfer, 53, 537–551.

Hussain S, Jamal M, Ahmed S E, (2019). Hydrodynamic forces and heat transfer of nanofluid forced convection flow around a rotating cylinder using finite element method: The impact of nanoparticles. International Communications in Heat and Mass Transfer, 108, 104310.

Jamaludin A, Nazar R, Naganthran K, Pop I, (2021). Mixed convection hybrid nanofluid flow over an exponentially accelerating surface in a porous media. Neural Computing and Applications, 33, 15719-15729.

Jamshed W, Eid M R, Hussain S M, Abderrahmanee A, Safdar R, Younis O, Pasha A A, (2022). Physical specifications of MHD mixed convective of Ostwald-de Waele nanofluids in a vented-cavity with inner elliptic cylinder. International Communications in Heat and Mass Transfer, 134, 106038.

Kefayati G H R, (2015). Mesoscopic simulation of mixed convection on non-Newtonian nanofluids in a two sided lid-driven enclosure. Advanced Powder Technology, 26, 576-588.

Kefayati G H R, (2016). Simulation of double diffusive MHD (magnetohydrodynamic) natural convection and entropy generation in an open cavity filled with power-law fluids in the presence of Soret and Dufour effects (Part I: Study of fluid flow, heat and mass transfer). Energy, 107, 889-916.

Koca A, Oztop H F, Varol Y, (2007). The effects of Prandtl number on natural convection in triangular enclosures with localized heating from below. International Communications in Heat and Mass Transfer, 34, 511-519.

Laidoudi H, Abderrahmane A, Saeed A M, Guedri K, Younis O, Marzouki R, Chung J D, Shah N A, (2022b). Lid-driven chamber with 3D elliptical obstacle under the impacts of the nano-properties of the fluid, Lorentz force, thermal buoyancy, and space porosity, Nanomaterials, 12, 2373.

Laidoudi H, (2020). Buoyancy-driven flow in annular space from two circular cylinders in tandem arrangement. Metallurgical and Materials Engineering, 26, 87-102.

Laidoudi H, Ameur H, Sahebi S A R, Hoseinzadeh S, (2022a). Thermal analysis of steady simulation of free convection from concentric elliptical annuli of a horizontal arrangement. Arabian Journal for Science and Engineering, 47, 15647–15660.

Laidoudi H, Ameur H, (2020). Investigation of the mixed convection of power-law fluids between two horizontal concentric cylinders: Effect of various operating conditions, Thermal Science and Engineering Progress, 20, 100731.

Laidoudi H, Bouzit M, (2017a). The effect of asymmetrically confined circular cylinder and opposing buoyancy on fluid flow and heat transfer. Defect and Diffusion Forum, 374, 18-28.

Laidoudi H, Bouzit M (2017b). Mixed convection heat transfer from confined tandem circular cylinders in cross-flow at low Reynolds number, Mechanics, 23, 522-527.

Laidoudi H, Bouzit M, (2017c). Suppression of flow separation of power-law fluids flow around a confined circular cylinder by superimposed thermal buoyancy. Mechanics, 23, 220-227.

Laidoudi H, Bouzit M, (2018). Mixed convection in Poiseuille fluid from an asymmetrically confined heated circular cylinder. Thermal science, 22, 821-834.

Laidoudi H, Helmaoui M, Bouzit M, Ghenaim A, (2021). Natural-convection of Newtonian fluids between two concentric cylinders of a special cross-sectional form, Thermal Science, 25, 3701-3714.

Liao C C, Lin C A, (2012). Influences of a confined elliptic cylinder at different aspect ratios and inclinations on the laminar natural and mixed convection flows. International Journal of Heat and Mass Transfer, 55, 6638-6650.

Luo K, Yi H L, Tan H P, (2014). Coupled Radiation and Mixed Convection in an Eccentric Annulus Using the Hybrid Strategy of Lattice Boltzmann-Meshless Method. Numerical Heat Transfer, Part B, 66, 243-267.

Lorenzini G, Machado B S, Isoldi L A, dos Santos E D, Rocha LA O, (2016). Constructal design of rectangular fin intruded into mixed convective lid-driven cavity flows. Journal of Heat and Mass Transfer, 138, 102501.

Mahdy A, (2010). Soret and Dufour effect on double diffusion mixed convection from a vertical surface in a porous medium saturated with a non-Newtonian fluid. Journal of Non-Newtonian Fluid Mechanics,165, 568-575.

Mandal D K, Biswas N, Manna N K, Gorla R S R, Chamkha A J, (2023). Hybrid nanofluid magnetohydrodynamic mixed convection in a novel W-shaped porous system. International Journal of Numerical Methods for Heat & Fluid Flow, 33, 510-544.

Matin M H, Pop I, Khanchezar S, (2013). Natural convection of power-law fluid between two-square eccentric duct annuli. Journal of Non-Newtonian Fluid Mechanics, 197, 11-23.

Molla M M, Yao L S, (2009). Mixed convection of non-Newtonian fluids along a heated vertical flat plate. International Journal of Heat and Mass Transfer, 52, 3266-3271.

Mokeddem M, Laidoudi H, Makinde OD, Bouzit M (2019). 3D Simulation of incompressible poiseuille flow through 180 curved duct of square cross-section under effect of thermal buoyancy, Periodica Polytechnica Mechanical Engineering, 63, 257–269.

Prhashanna A, Chhabra RP, (2010). Free convection in power-law fluids from a heated sphere. Chemical Engineering Science, 65, 6190-6205.

Sadr AN, Shekaramiz M, Zarinfar M, Esmaily A, Khoshtarash H, Toghraie D, (2022). Simulation of mixed-convection of water and nano-encapsulated phase change material inside a square cavity with a rotating hot cylinder. Journal of Energy Storage, 47, 103606.

Sarris I, Zikos G, Grecos A, Vlachos N, (2006). On the limits of validity of the low magnetic Reynolds number approximation in MHD natural-convection heat transfer. Numerical Heat Transfer, Part B, 50, 158-180.

Selimefendigil F, Öztop H F, (2018). Mixed convection of nanofluids in a three dimensional cavity with two adiabatic inner rotating cylinders. International Journal of Heat and Mass Transfer, 117, 331-343.

Sheikholeslami M, Hayat T, Alsaedi A, (2016). MHD free convection of Al2O3–water nanofluid considering thermal radiation: A numerical study. International Journal of Heat and Mass Transfer, 96, 513-524.

Sheikholeslami M, Oztop HF, (2017). MHD free convection of nanofluid in a cavity with sinusoidal walls by using CVFEM. Chinese Journal of Physics, 55, 2291-2304.

Torres J F, Ghanadi F, Wang Y, Arjomandi M, Pye J, (2020). Mixed convection and radiation from an isothermal bladed structure. International Journal of Heat and Mass Transfer, 147, 118906.

Yadav C K, Dey K, Manna N K, Biswas N, (2022). Low Reynolds number MHD mixed convection of nanofluid in a corner heated grooved cavity. Materials Today: Proceedings, 63, 170-175.

Yuce B E, Pulat E, (2018). Forced, natural and mixed convection benchmark studies for indoor thermal environments. International Communications in Heat and Mass Transfer, 92, 1-14.

Zhang T, Che D, (2016). Double MRT thermal lattice Boltzmann simulation for MHD natural convection of nanofluids in an inclined cavity with four square heat sources. International Journal of Heat and Mass Transfer, 94, 87-100.